HHS Public Access

Author manuscript

Bioorg Med Chem Lett. Author manuscript; available in PMC 2018 June 01.

Published in final edited form as:

Bioorg Med Chem Lett. 2017 June 01; 27(11): 2432–2438. doi:10.1016/j.bmcl.2017.04.011.

Design, synthesis, and X-ray structural studies of BACE-1 Inhibitors containing substituted 2-oxopiperazines as P1′-P2′ ligands

Arun K. Ghosh[*,a,b], **Margherita Brindisi**[a], **Yu-Chen Yen**[c], **Emilio L. Cárdenas**[a], **Jean-Rene Ella-Menye**[a], **Nagaswamy Kumaragurubaran**[a], **Xiangping Huang**[d], **Jordan Tang**[d,e], and **Andrew D. Mesecar**[a,c,f]

[a]Department of Chemistry, Purdue University, West Lafayette, IN 47907

[b]Department of Medicinal Chemistry, Purdue University, West Lafayette, IN 47907

[c]Department of Biological Sciences, Purdue University, West Lafayette, IN 47907

[d]Protein Studies Program, Oklahoma Medical Research Foundation

[e]Department of Biochemistry and Molecular Biology, University of Oklahoma Health Science Center, Oklahoma City, OK 73104

[f]Department of Biochemistry, Purdue University, West Lafayette, IN 47907

Abstract

We report the design and synthesis of a series of BACE1 inhibitors incorporating mono-and bicyclic 6-substituted 2-oxopiperazines as novel P1′ and P2′ ligands and isophthalamide derivative as P2-P3 ligands. Among mono-substituted 2-oxopiperazinones, inhibitor **5a** with *N*-benzyl-2-oxopiperazinone and isophthalamide showed potent BACE1 inhibitory activity (K_i = 2 nM). Inhibitor **5g**, with *N*-benzyl-2-oxopiperazinone and substituted indole-derived P2-ligand showed a reduction in potency. The X-ray crystal structure of **5g**-bound BACE1 was determined and used to design a set of disubstituted 2-oxopiperazinones and bicyclic derivatives that were subsequently investigated. Inhibitor **6j** with an oxazolidinone derivative showed a BACE1 inhibitory activity of 23 nM and cellular EC_{50} of 80 nM.

Graphical abstract

A series of BACE1 inhibitors incorporating mono- and bicyclic 2-oxopiperazines is described. Inhibitor **5a** showed an enzyme K_i of 2 nM and a cellular EC_{50} value of 3.5 nM. An X-ray structural analysis of a realted compound **5g**-bound BACE1 provided insight into the ligand-binding site interactions.

[*]Corresponding author. Tel.: +1-765-494-5323; fax: +1-765-496-1612; akghosh@purdue.edu (AKG).

Supplementary data

Supplementary data associated with this article can be found in the online version.

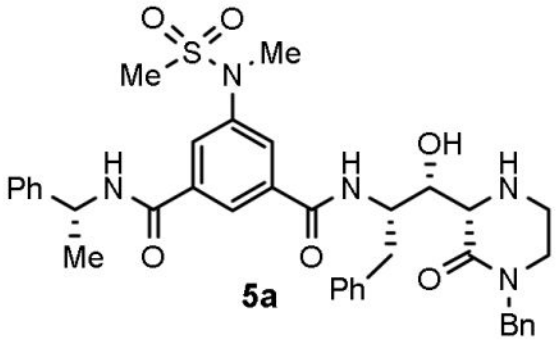

5a

Keywords

BACE-1; β-secretase; Alzheimer's disease; Memapsin 2; Protease inhibitors; design; piperazinones; inhibitor; secretase

Alzheimer's disease (AD) continues to be a major healthcare challenge in medicine.[1,2] Currently, there is no effective treatment that will prevent or slow down the progression of AD.[3,4] In recent years, a significant effort is being devoted toward the development of β-secretase inhibitors as potential drugs for AD treatment.[5,6] There are at least three β-secretase (also known as memapsin 2 or BACE1) inhibitors that have entered advanced clinical trials.[7] The pathological hallmark of AD has been the accumulation of β-amyloid (Aβ) peptides in the brain. This results in the accumulation of amyloid plaques and neurofibrillary tangles which leads to neuronal cell death.[8,9,10]

One of the major goals of today's AD drug discovery efforts is to reduce Aβ-production through the inhibition of β-secretase. Aβ is produced by the sequential cleavage of the amyloid precursor protein (APP) by two key aspartic acid proteases, first by the β-secretase (β-site APP cleaving enzyme) and then by a γ-secretase. There are two BACE isoforms that are designated as BACE1 (memapsin 2) and BACE2 (memapsin 1). BACE1 (memapsin 2) is involved in the amyloidogenic pathway and is responsible for cleaving APP leading to the formation of 40/42 residue peptides, the major constituent of the brain amyloid plaques.[11–13] Thus, development of potent and selective BACE1 inhibitors has become a major focus for AD drug discovery in many laboratories due to the central role of BACE1 in APP processing. Also, it is encouraging that BACE1 gene deletion in mice showed only a mild phenotypic response. It is important to note that recent studies revealed that besides APP, BACE has other important substrates.[14,15]

Over the years, many potent and selective BACE1 inhibitors have been developed based upon hydroxyethylene and hydroxyethylamine transition-state isosteres.[5,13] We and others have reported BACE1 inhibitors incorporating substituted isophthalamides as P2-P3 ligands in combination with hydroxyethylene and hydroxyethylamine isosteres.[16–19] As shown in Figure 1, BACE1 inhibitors **1** and **2** showed excellent BACE1 potency with low nM K_i values and they also showed reduction of cellular Aβ production. Our X-ray structural studies of inhibitors **1**- and **2**-bound BACE1 provided insight into the ligand-binding site interactions. In particular, the P2-isophthalamide derivative occupies the S2-site and makes

extensive hydrogen bonding interactions with Asn 233, Ser 325, and Arg 235.[19,20,21] The phenylmethyl moiety makes non-polar interactions with the extended hydrophobic binding site. We have subsequently designed a number of other potent and selective BACE1 inhibitors, including inhibitor **3** with a substituted isophthalamide ligand.[13,19,21] Substituted isophthalamide derivatives without the 5-methylsulfonamides have also been utilized in the design of potent BACE1 inhibitors with hydroxyethylamine isosteres.[5,13] Cumming and co-workers designed a series of BACE1 inhibitors incorporating conformationally constrained piperazine and piperazinone derivatives as the P1′ and P2′ ligands while keeping the basic hydroxyethylamine scaffold as the transition-state mimic.[22,23,24] As shown in Figure 2, they have investigated dipropyl isophthalamide as the P2-ligand in combination with mono-substituted piperazinones.

In our continuing efforts toward BACE1 inhibitor design, we are interested in the incorporation of classical transition state isosteres embedded in many FDA approved HIV-1 protease inhibitors.[25–27] In the present studies, we have investigated various di- and tri-substituted piperazinone-derived hydroxyethylamine isosteres in combination with P2-P3 isophthalamide ligands shown in inhibitors **1** and **2**. Herein, we report the design, synthesis, and evaluation of a series of BACE1 inhibitors with substituted piperazinones with donor and acceptor groups to interact with the S1′-S2′ subsites of the BACE1 active site. We opted to utilize the isophthalamide P2-P3 ligand that we have successfully incorporated in previous inhibitors. Asymmetric synthesis of these substituted piperazinones and aldol reaction with phenylalaninal provided convenient access to various piperazinone-derived hydroxylethylamine isosteres.

Initially, we focused our investigation on a small set of P2′ ligands. In particular, we explored the outcome of diverse alkyl substituents on the nitrogen of the oxopiperazine ring (Figure 2, structure class **5**). We then focused on the incorporation of substituents at the C6-position of the oxopiperazine ring to modulate inhibitor binding at the S1′-subsite. Furthermore, we planned to explore reduction of the oxopiperazine carbonyl group and incorporation of a bicyclic ring involving R_1 and R_2 groups (Figure 2, structure class **6**). The synthesis of inhibitors **5a–f** is shown in Scheme 1. We carried out an aldol reaction between (*S*)-*N,N*-dibenzylphenylalaninal **7a** and commercially available substituted 4-Boc-2-oxopiperazines **8a–f**.[28,29] As a representative example, for compound **9a**, oxopiperazine **8a**[28] in THF was treated with 1.5 equivalents of LHMDS at −78 °C and the reaction mixture was stirred for 2 h. *N,N*-dibenzylphenylalaninal **7a** was then added and the resulting mixture was warmed to 23 °C for 3 h. The reaction was quenched with aqueous $NaHCO_3$ solution, then a standard work up and chromatography over silica gel provided **9a** in 46% yield as a pure isomer.[16] Other oxopiperazines **8b–f** were converted to aldol products **9b–f** in similar yields (40–46%). The stereochemical assignment of aldol products was based upon literature precedence.[16,29,30] The removal of the *N,N*-dibenzyl groups by catalytic hydrogenation over Pearlman's catalyst afforded the corresponding amines **10a–f** in very good yields (85–90%). Amines **10a–f** were coupled with known substituted isophthalic acid derivative **11**[19] in CH_2Cl_2 in the presence of EDCI, HOBt, and diisopropylethylamine (DIPEA), which afforded inhibitors **5a–f** in good yields. For the synthesis of inhibitor **5g**, substituted indole carboxylic acid **12** was prepared as described previously.[31] Coupling of amine **10a** with acid

12 provided the corresponding coupling product. Removal of the Boc-group by exposure to TFA in CH_2Cl_2 afforded inhibitor **5g** in 60% yield for the two steps.

Besides *N*-substituted oxopiperazines, we also planned to explore *N*-alkyl-6-substituted 2-oxopiperazines. Previous literature reports[32,33] for the synthesis of these substituted oxopiperazine, involved low-yielding coupling reactions or harsh reaction conditions. We therefore designed an improved route using readily available amino acids as shown in Scheme 2. (*S*)-*N,N*-dibenzylphenylalaninal **7a** and (*S*)-*N,N*-dibenzylalaninal **7b** were prepared from the corresponding alcohol as described previously.[29] Reductive amination[34] of these aldehydes with glycine ethyl ester hydrochloride with $Na(OAc)_3BH$ in a mixture of acetic acid and 1,2-dichloroethane at 23 °C for 10 h provided the corresponding amines. These were protected as Boc-derivatives **13a** and **13b** by treatment with Boc_2O and triethylamine in MeOH. Catalytic hydrogenation of **13a,b** over Pearlman's catalyst in ethanol in the presence of AcOH at 23 °C afforded the corresponding amines. Treatment of the resulting aminoester with NaH and benzylbromide in THF at 23 °C furnished *N*-benzyl 6-alkyl-2-oxopiperazines **14a,b** in good yields. The synthesis of enantiomeric 2-oxopiperazines *ent*-**14a,b** were carried out using analogous procedures utilizing (*R*)-*N,N*-dibenzylphenylalaninal *ent*-**7a** or (*S*)-*N,N*-dibenzylalaninal *ent*-**7b**. For the synthesis of 2-oxo-piperazine **15**, amino ester derivative *ent*-**13a** was hydrogenated over Pearlman's catalyst and the resulting amino ester was treated with NaH and methyl iodide in THF at 23 °C to provide **15** in 68% yield over two-steps.

The synthesis of the 6-substituted-2-oxopiperazine-derived inhibitors is shown in Scheme 3. Aldol reaction of substituted-2-oxopiperazines **14a,b** with (*R*)-*N,N*-dibenzylphenylalaninal **7** provided the corresponding aldol products in moderate yields (38–45%). The absolute and relative stereochemistry of the hydroxyl group and cyclic piperazinone ring were unambiguously set via chirality transfer from the α-amino acid center in a non-chelation controlled aldol reaction as described previously.[16,29,30] Catalytic hydrogenation of these aldol products provided amines **16a,b**. Coupling of amines **16a,b** with isophthalamide derivative **11** in the presence of EDCI, HOBt in CH_2Cl_2 afforded the corresponding coupling products in good yields (55–60%). Exposure of these coupling products to TFA in CH_2Cl_2 at 23 °C afforded inhibitors **6a,b**. Inhibitors **6c–i** were prepared by aldol reaction of aldehyde **7** and 6-substituted-2-oxopiperazines *ent*-**14a,b** and **15** followed by the conversion of the resulting aminoalcohols **17a–c** to inhibitors **6c–f** following a similar reaction sequence as described above. For the synthesis of inhibitor **6g**, known[17,22] 3-(dipropylcarbamoyl)-5-methylbenzoic acid **18** was coupled with amine **17a** and the resulting product was treated with TFA in CH_2Cl_2 to provide **6g** in 67% yield for the two steps.

Synthesis of bicyclic piperazinone-derived compound **6h** is shown in Scheme 4. Cbz-protected (*R*)-prolinal **19** was employed as the starting material. Reductive amination of **19** with glycine ethyl ester provided amine **20**. *N*-Boc protection with Boc_2O afforded Boc-derivative **21.** Catalytic hydrogenation of **21** over Pearlman's catalyst provided the corresponding amine which was concommitantly cyclized to bicyclic derivative **22**. Aldol reaction of **22** with aldehyde **7a** provided aldol product **23** which was converted to final

compound **6h** as described above. Compound **6i** was similarly obtained starting from Cbz-protected (*S*)-prolinal.

Synthesis of oxazolidinone-derived BACE1 inhibitor **6j** is shown in Scheme 5. Aminoalcohol derivative **24** was prepared from aldol reaction of a suitable oxopiperazine and aldehyde **7a** as described above. The lactam carbonyl was reduced by treatment with borane-dimethyl sulfide complex in THF at reflux to provide amine derivative **25.** Catalytic hydrogenation of **25** over Pearlman's catalyst provided the corresponding amine which was coupled with isophthalic acid derivative **11** to provide the corresponding amide coupling product. Treatment of this product with TBAF in THF removed the TBS-group and provided aminoalcohol **26**. Exposure of **26** to 1,1-carbonyldiimidazole in dioxane at reflux for 36 h afforded the corresponding oxazolidinone product. Treatment of the resulting oxazolidinone with TFA in CH_2Cl_2 at 23 °C for 1.5 h afforded inhibitor **6j** in excellent yield.

The structures and BACE1 inhibitory activity of various inhibitors containing *N*-alkyl piperazinones are shown in Table 1. The BACE-1 inhibitory activity of **5a–g** was determined against recombinant enzyme using our previously reported assay protocols.[35–37] As can be seen, the size and electronic effects on the *N*-alkyl derivatives are important for potency. Compound **5a** with *N*-benzyl substituent is significantly more potent than compound **5b** with an *N*-isobutyl derivative (entries 1 and 2). A small linear chain proproyl derivative **5c** is less potent than **5a** and **5b**. We incorporated an electron rich OMe group at the *para*, *meta,* and *ortho* position of the phenyl ring on inhibitor **5a**. The resulting inhibitors, **5d**, **5e**, and **5f**, showed significant reductions in potency. Incorporation of a substituted indole carboxamide as the P2 ligand in place of the isophthalamide provided inhibitor **5g**. However, this inhibitor showed a reduction in potency compared to isophthalamide derivative **5a.** Inhibitor **5g** displayed enhanced BACE2 selectivity with a K_i =7.14 μM for BACE2.

To obtain molecular insight into the inhibitor-BACE1 interactions, we determined the X-ray structure of **5g** bound to BACE1 to 2.2 Å resolution (R_{Free} = 0.192, R_{work} = 0.16).[38] As shown in Figure 3, the transition-state hydroxyl group forms a tight hydrogen bond with one of the catalytic aspartates Asp32. The 2-oxopiperazinone moiety fits nicely in the S1′ and S2′ subsites. The C2-carbonyl oxygen appears to form a strong hydrogen bond with the Thr72-backbone amide hydrogen. The P2-indole ligand makes a number of interactions in the active site including the formation of a pair of hydrogen bonds between one of the oxygen atoms of the sulfonamide group and the backbone amide hydrogens of Thr232 and Asn233. The benzyl group fits into a hydrophobic pocket formed by Leu 30, Tyr 71 and Trp 115 shown in Figure 4.

The *N*-benzyl group also fits into a hydrophobic pocket formed from residues Ser35, Val69, Pro 70, Tyr 71, Ile126 and Tyr198 (Figure 4) and provides critical data on the molecular interactions of *N*-benzylpiperazinone in the S2′ site of the active site. It appears that the unsubstituted *N*-benzyl group is quite optimum for this hydrophobic pocket. Further increases in steric bulk by incorporating methoxy group likely change the conformation of the oxapiperazinone's carbonyl group and destabilizes the hydrogen bond interaction with the Thr 72 flap residue's backbone -NH group (Figure 3). This may explain significant loss of potency for the methoxybenzyl derivatives compound to benzyl derivative **5a**. Since

inhibitor **5a** with a P2-isophthalamide derivative and P2′-*N*-benzylpiperazinone showed the best potency, we decided to further modify the piperazinone scaffold with a combination of a various *N*-alkyl and 6-alkyl substituted 2-piperazinones. The structures and potency of a set of disubstituted 2-piperazinone-derived inhibitors **6a–j** are shown in Table 2.

As can be seen, the set of 6-substituted-piperazinone- and piperazine-containing compounds show well-defined structure-activity relationships (SARs). First of all, the stereochemistry at the 6-position was found to be critical to inhibitory activity, as demonstrated by the dramatic difference in potency between compounds **6a** and **6b** (K_i = 52.9 μM vs K_i = 180 nM respectively). The removal of the lactam carbonyl oxygen in **6c** resulted in a reduction of potency. Beyond the preference for the (*R*)-configuration at 6-position, the preference for a small alkyl group is also highlighted (**6b** *vs* **6e**, K_i = 175.5 nM *vs* K_i = 222 μM, respectively). Inhibitor **6f** with a combination of *N*-Me and 6-(*R*)-benzyl piperazinone displayed best inhibitory activity. Incorporation of *N*,*N*-dipropyl isophthalamide derivative in inhibitor **6g** resulted in a significant loss of potency (K_i = 320 nM vs K_i = 12 nM) compared to *N*-methyl sulfonamide-derivatives as the P2-ligand. We then designed a set of bicyclic P1′ and P2′ ligands in inhibitors **6h–6j**. Inhibitor **6h** with C-6(*R*) stereochemistry is significantly more potent than inhibitor **6i** with 6-(*S*)-stereochemistry. The oxazolidinone derivative **6j** displayed comparable potency to inhibitor **6h**.

We measured the potency of a subset of inhibitors in different assays. Regarding the first series of inhibitors **5a–g**, we sought to determine the cell activity of the representative compound **5a**, bearing the P2-isophthalamide derivative and the P2′ *N*-benzylpiperazinone. Inhibitor **5a** displayed an EC_{50} value of 3.5 nM in a cell-based assay. Also, we assessed the cellular outcome for compound **5g**, in order to appraise the contribution of the substituted indole carboxamide as the P2 ligand. Compound **5g** showed an EC_{50} value of 18.5 nM. For the prototype of the series **5a** we also evaluated the selectivity over β-site APP-cleaving enzyme 2 (BACE2), for its close similarity to BACE1, and cathepsin D (CatD), for its ubiquitous presence in nearly all the cells. Compound **5a** showed marginal selectivity against BACE2 (K_i = 134 nM) and good selectivity against CatD (K_i = 1.5 μM). We also evaluated the BACE2 inhibitory activity of compound **5g**, which showed improved selectivity (BACE2 K_i = 7.14 μM). Finally, we sought to compare the cell-based activity of two bicyclic inhibitors, namely the bicyclic piperazinone inhibitor **6g** and the oxazolidinone derivative **6i**, displaying comparable enzyme inhibitory potency. Inhibitor **6g** showed an EC_{50} of 184 nM, while inhibitor **6j** is slightly more potent in the same settings (EC_{50} = 80 nM).

In summary, we have designed and synthesized a series of BACE1 inhibitors containing substituted 2-oxopiperazines as the P1′ and P2′ ligands and substituted isophthalamide as the P2 ligand. We have developed methodologies for the synthesis of 6-alkyl and *N*-alkyl piperazinones, as well as bicyclic piperazinones. Among the *N*-substituted piperazinones examined, *N*-benzyl derivative **5a** showed the best result. The choice of substitution on the isophthalamide is critical to potency. The combination of *N*-alkyl and 6-alkyl is important and the stereochemistry at the 6-alkyl position is also critical. Inhibitors **6f** with *N*-methyl and 6-benzyl derivatives provided best BACE1 activity. Also, bicyclic piperazinone **6g** and

oxazolidinone derivative **6i** showed good BACE1 inhibitory activity as well as inhibition of cellular production of Aβ in neuroblastoma cells. We determined the X-ray structure of inhibitor **5g**-bound BACE1 to 2.2Å resolution. The structure provided important molecular insight into the ligand-binding site interactions in the S1′ and S2′ subsites of β-secretase. Further design and improvement of inhibitor properties are in progress.

Supplementary Material

Refer to Web version on PubMed Central for supplementary material.

Acknowledgments

Financial support by the National Institutes of Health and the Purdue University Office of the Executive Vice President for Research are gratefully acknowledged. We would also like to thank Dr. Kalapala Venkateswara Rao for helpful discussions. BACE1 crystallization, NMR and Mass Spectrometry were all performed using shared resources that are partially supported by the Purdue Center for Cancer Research through NIH grant (P30CA023168). This research used resources of the Advanced Photon Source, a U.S. Department of Energy (DOE) Office of Science User Facility operated for the DOE Office of Science by Argonne National Laboratory under Contract No. DE-AC02-06CH11357. Use of the Lilly Research Laboratories Collaborative Access Team (LRL-CAT) beamline at Sector 31 of the Advanced Photon Source was provided by Eli Lilly Company, which operates the facility.

References and notes

1. Alzheimer's Association. Alzheimer's Disease Facts and Figures. 2016. Available at: www.alz.org/alzheimers_disease_facts_figures.asp
2. Rutten BP, Steinbusch HW. Mol Neurodegener. 2013; 8:33. [PubMed: 24148188]
3. Lansdall CJ. Bioscience Horizons. 2014; 7:1–11.
4. Prince M, Bryce R, Albanese E. Alzheimer's and Dementia. 2013; 9:63–75.
5. Ghosh AK, Osswald HL. Chem Soc Rev. 2014; 43:6765–6813. [PubMed: 24691405]
6. Vassar R, Kovacs DM, Yan R, Wong PC. J Neurosci. 2009; 29:12787–12794. [PubMed: 19828790]
7. Vassar R. Alzheimer's Res Ther. 2014; 6:89. [PubMed: 25621019]
8. Tanzi RE. Cold Spring Harb Perspect Med. 2012:2.
9. Selkoe DJ, Schenk D. Annu Rev Pharacol. 2003; 43:545–584.
10. Hardy J, Selkoe DJ. Science. 2002; 297:353–356. [PubMed: 12130773]
11. Evin G, Barakat A, Masters CL. Internat J Biochem & Cell Biology. 2010; 42:1923–1926.
12. Citron M. Trends in Pharmacological Sciences. 2004; 25:92–97. [PubMed: 15102495]
13. Ghosh AK, Brindisi M, Tang J. J Neurochem. 2012; 120(Suppl 1):71–83. [PubMed: 22122681]
14. Luo Y, Bolon B, Kahn S, Bennett BD, Babu-Khan S, Denis P, Fan W, Kha H, Zhang J, Gong Y, Martin L, Louis JC, Yan Q, Richards WG, Citron M, Vassar R. Nature Neuroscience. 2001; 4:231–232. [PubMed: 11224535]
15. Cai H, Wang Y, McCarthy D, Wen H, Borchelt DR, Price DL, Wong PC. Nature Neuroscience. 2001; 4:233–234. [PubMed: 11224536]
16. Cumming JN, Le TX, Babu S, Carroll C, Chen X, Favreau L, Gaspari P, Guo T, Hobbs DW, Huang Y, Iserloh U, Kennedy ME, Kuvelkar R, Li G, Lowrie J, McHugh NA, Ozgur L, Pan J, Parker EM, Saionz K, Stamford AW, Strickland C, Tadesse D, Voigt J, Wang L, Wu Y, Zhang L, Zhang Q. Bioorg Med Chem Lett. 2008; 18:3236–3241. [PubMed: 18468890]
17. Cumming JN, Babu S, Huang Y, Carroll C, Chen X, Favreau L, Greenlee W, Guo T, Kennedy ME, Kuvelkar R, Le T, Li G, McHugh NA, Orth P, Ozgur L, Parker EM, Saionz K, Stamford AW, Strickland C, Tadesse D, Voigt J, Zhang L, Zhang Q. Bioorg Med Chem Lett. 2010; 20:2837–2842. [PubMed: 20347593]
18. Stachel SJ, Coburn CA, Steele TG, Jones KG, Loutzenhiser EF, Gregro AR, Rajapakse HA, Lai MT, Crouthamel MC, Xu M, Tugusheva K, Lineberger JE, Pietrak BL, Espeseth AS, Shi XP,

Chen-Dodson E, Holloway MK, Munshi S, Simon AJ, Kuo L, Vacca JP. J Med Chem. 2004; 47:6447–6450. [PubMed: 15588077]

19. Ghosh AK, Kumaragurubaran N, Hong L, Kulkarni S, Weerasena V, Turner R, Koelsch G, Bilcer G, Tang J. J Med Chem. 2007; 50:2399–2407. [PubMed: 17432843]
20. Ghosh AK, Kumaragurubaran N, Hong L, Kulkarni S, Xu X, Miller HB, Reddy DS, Weerasena V, Turner R, Chang W, Koelsch G, Tang J. Bioorg Med Chem Lett. 2008; 18:1031–1036. [PubMed: 18180160]
21. Ghosh AK, Kumaragurubaran N, Hong L, Lei H, Hussain KA, Liu CF, Devasamudram T, Weerasena V, Turner R, Koelsch G, Bilcer G, Tang J. J Am Chem Soc. 2006; 128:5310–5311. [PubMed: 16620080]
22. Iserloh U, Wu Y, Cumming JN, Pan J, Wang LY, Stamford AW, Kennedy ME, Kuvelkar R, Chen X, Parker EM, Strickland C, Voigt J. Bioorg Med Chem Lett. 2008; 18:414–417. [PubMed: 18023580]
23. Maillard MC, Hom RK, Benson TE, Moon JB, Mamo S, Bienkowski M, Tomasselli AG, Woods DD, Prince DB, Paddock DJ, Emmons TL, Tucker JA, Dappen MS, Brogley L, Thorsett ED, Jewett N, Sinha S, John V. J Med Chem. 2007; 50:776–781. [PubMed: 17300163]
24. Iserloh, U., Cummins, JN. Peptidomimetic BACE1 Inhibitors for Treatment of Alzheimer's Disease: design and evolution in Aspartic Acid proteases as Therapeutic Targets. Ghosh, AK., editor. Wiley-VCH; 2010. p. 441-479.
25. Virgil, S. First Generation HIV-1 Protease Inhibitors for the treatment of HIV/AIDS. In: Ghosh, AK., editor. Aspartic Acid proteases as Therapeutic Targets. Wiley-VCH; 2010. p. 139-168.
26. Ghosh, AK., Chapsal, B. Second-Generation Approved HIV Protease Inhibitors for the Treatment of HIV/AIDS. In: Ghosh, AK., editor. Aspartic Acid proteases as Therapeutic Targets. Wiley-VCH; 2010. p. 169-204.
27. Ghosh AK, Osswald HL, Prato G. J Med Chem. 2016; 59:5172–5208. [PubMed: 26799988]
28. Bernotas RC, Adams G. Tetrahedron Lett. 1996; 37:7339–7342.
29. Reetz MT, Drewes MW, Schmitz A. Angew Chem Int Ed. 1987; 26:1141–1143.
30. Reetz MT. Chem Rev. 1999; 99:1121–1162. [PubMed: 11749442]
31. Ghosh AK, Rao KV, Yadav ND, Anderson DD, Gavande N, Huang X, Terzyan S, Tang J. J Med Chem. 2012; 55:9195–9207. [PubMed: 22954357]
32. Boger DL, Goldberg J, Satoh S, Ambroise Y, Cohen SB, Vogt PK. Helv Chim Acta. 2000; 83:1825–1845.
33. Whitby LR, Lee AM, Kunz S, Oldstone MBA, Boger DL. 2009; 19:3771–3774.
34. Abdel-Magid AF, Mehrman SJ. Org Process Res. 2006; 10:971–1031.
35. BACE1 inhibition was measured using recombinant enzyme produced from *E. coli* expression as described in reference 36. A fluorogenic substrate Arg-Glu(EDANS)-Glu-Val-Asn-Leu-Asp-Ala-Glu-Phe-Lys (Dabcyl)-Arg was used with 0.47 μM of the enzyme in 0.1 M Na-acetate + 5% dimethylsulfoxide, pH 4.5 at 37 °C. The excitation wavelength was 350 nm and the emission wavelength was 490 nm.
36. Lin X, Koelsch G, Wu S, Downs D, Dashti A, Tang J. Proc Natl Acad Sci, USA. 2000; 97:1456–1460. [PubMed: 10677483]
37. Ermolieff J, Loy JA, Koelsch G, Tang J. Biochem. 2000; 39:12450–12456. [PubMed: 11015226]
38. PDB code: 5VON. For details of X-ray studies, please see Supplementary information.

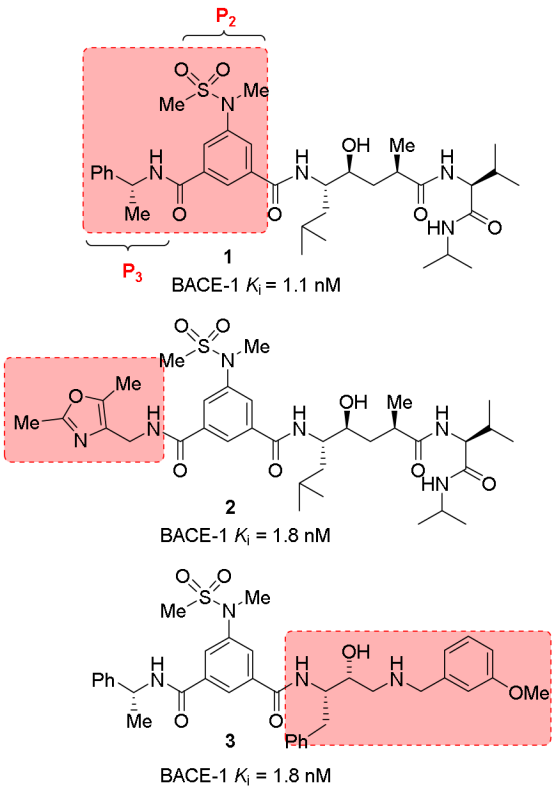

Figure 1.
BACE-1 inhibitors with isophthalamide P_2-P_3 ligands.

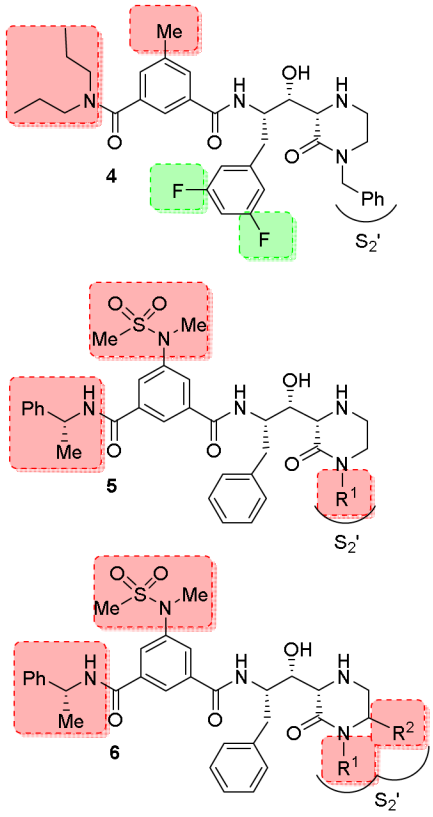

Figure 2.
Piperazinone and piperazine derivatives as BACE-1 inhibitors.

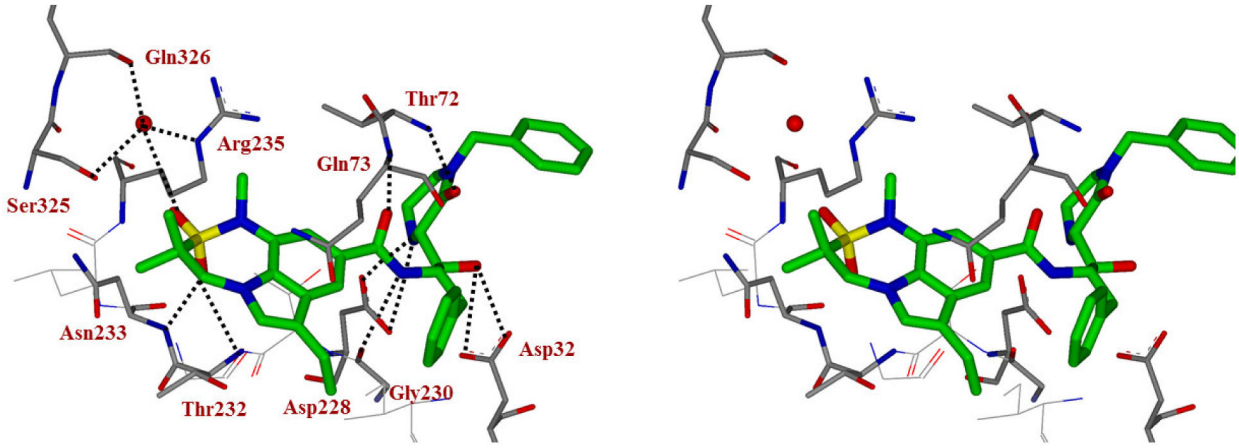

Figure 3.

Stereoview of the X-ray structure of inhibitor **5g** (green carbon chain) with BACE1 (PDB code: 5VON). Possible hydrogen bonds between the inhibitor and BACE1 are shown in black dotted lines.

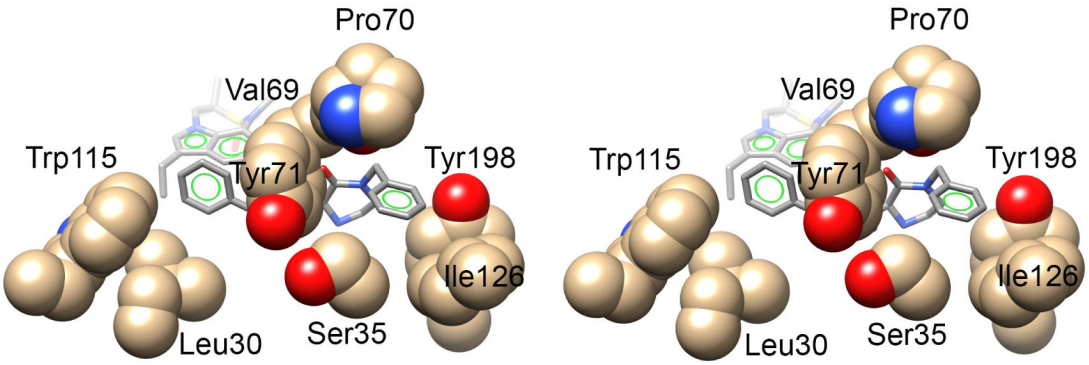

Figure 4.

Stereoview (Wall-eye) of the X-ray structure of BACE1 showing the two hydrophobic pockets that bind the benzyl and *N*-benzyl groups of inhibitor **5g** (PDB code: 5VON).

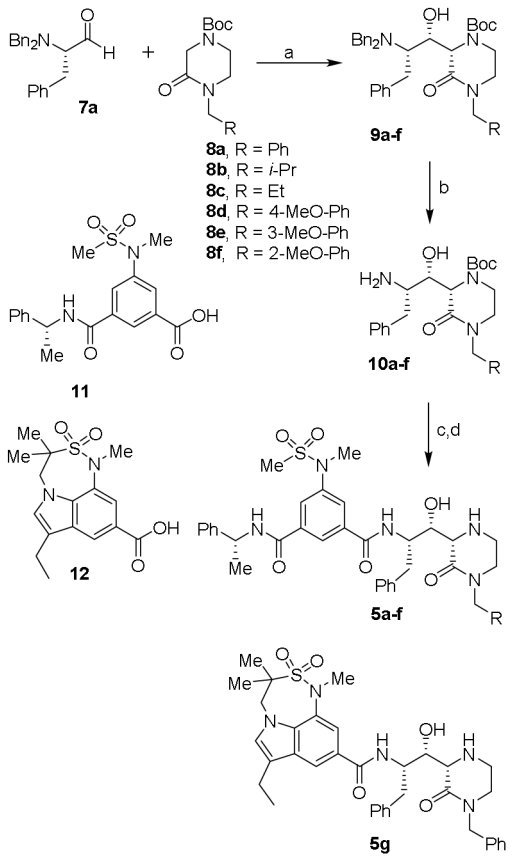

Scheme 1.

Reagents and conditions: (a) LHMDS, THF, −78 °C to 25 °C, 46%; (b) H_2, $Pd(OH)_2$, EtOH, AcOH, 23 °C, 90%; (c) **11**, or **12**, EDCI, HOBt, DIPEA, CH_2Cl_2; 23 °C, 60%; (d) TFA, CH_2Cl_2, 23 °C, 80%.

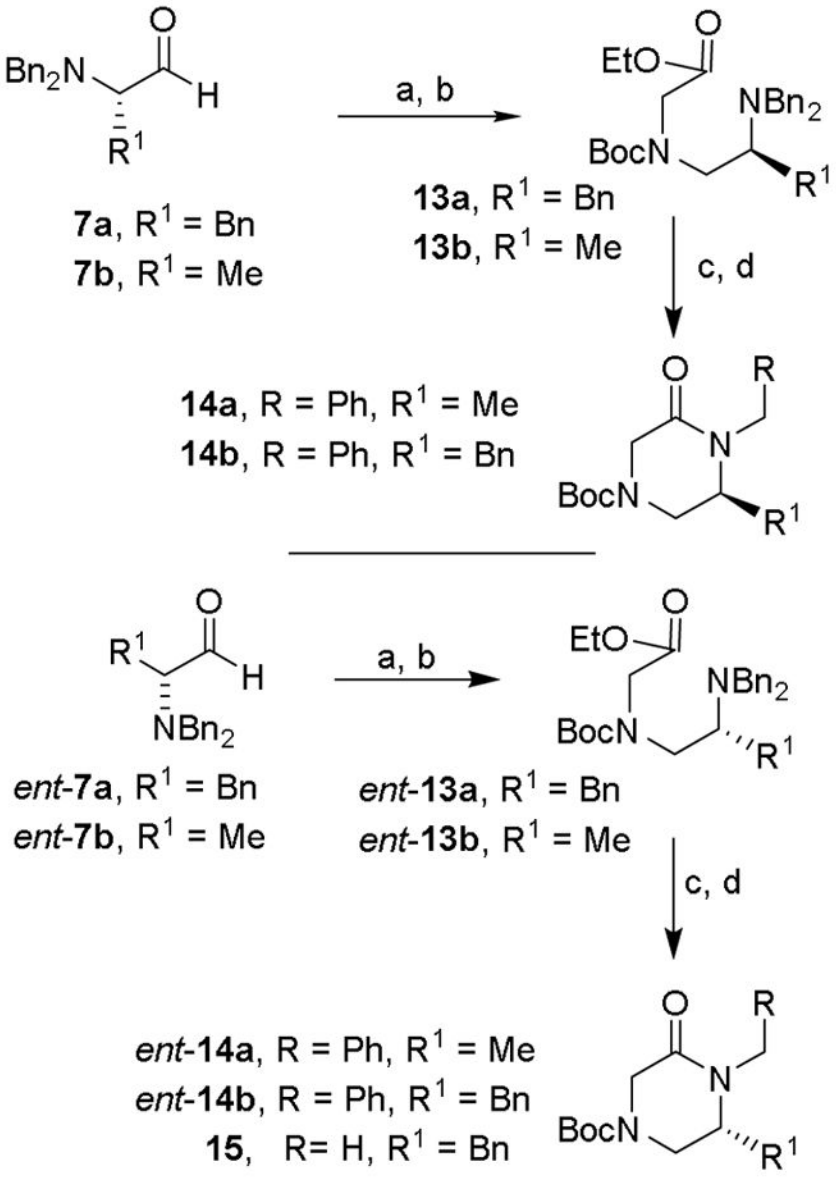

Scheme 2.

Reagents and conditions: (a) glycine ethyl ester hydrochloride salt, $NaBH(OAc)_3$, AcOH, 1,2-DCE, 23 °C, 85%; (b) Boc_2O, TEA, MeOH, 50 °C, 78%; (c) H_2, $Pd(OH)_2$, EtOH, AcOH, 23 °C; (d) BnBr or MeI, NaH, dry THF, 68% (over 2 steps).

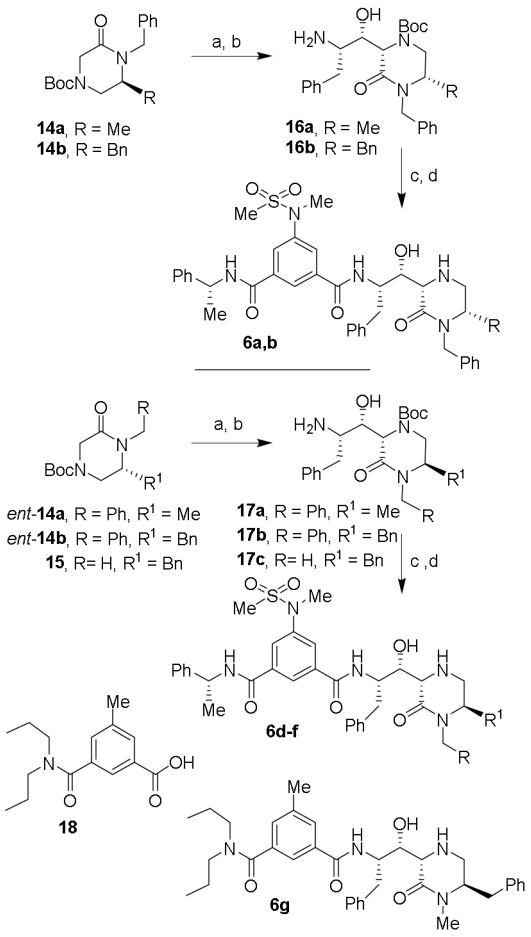

Scheme 3.

Reagents and conditions: (a) LHMDS, dry THF, −78 °C to 23 °C, then add aldehyde **7**, 38%; (b) H_2, $Pd(OH)_2$, EtOH, AcOH 23 °C; (c) **11** or **18**, EDCI, HOBt, DIPEA, CH_2Cl_2; 23 °C; (d) TFA, CH_2Cl_2, 23 °C, (31% over 3 steps); (e) BH_3•SMe, dry THF, reflux, 78%.

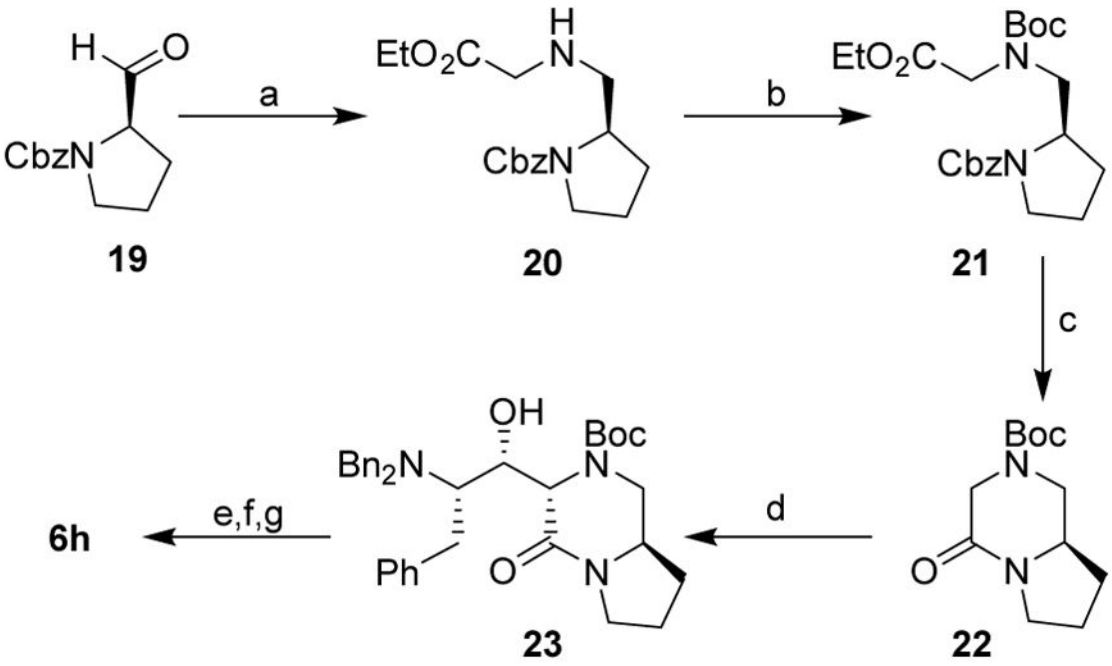

Scheme 4.

Reagents and conditions: (a) glycine ethyl ester hydrochloride salt, $NaBH(OAC)_3$, AcOH, 1,2-DCE, 25 °C, 80%; (b) Boc_2O, TEA, MeOH, 50 °C, 80%; (c) H_2, $Pd(OH)_2$, EtOH, AcOH, 25 °C, quant.; (d) **7a**, LHMDS, dry THF, −78 °C to 25 °C, 26%; (e) H_2, $Pd(OH)_2$, EtOH, AcOH, 25 °C; (f) **11**, EDCI, HOBt, DIPEA, CH_2Cl_2; 25 °C; (g) TFA, CH_2Cl_2, 25 °C, (30% over 3 steps).

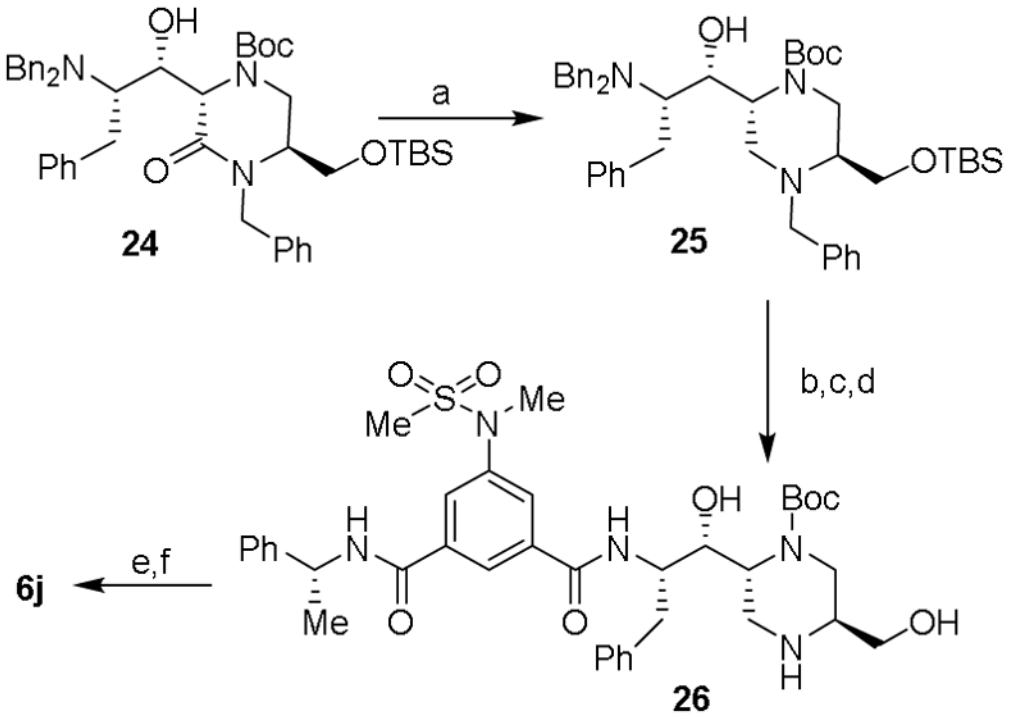

Scheme 5.

Reagents and conditions: (a) BH_3·SMe, dry THF, reflux, 84%; (b) **11**, EDCI, HOBt, DIPEA, CH_2Cl_2; 23 °C, 58%; (c) TBAF, THF, 0 °C to 23 °C, 2 h, 82%; (d) H_2, $Pd(OH)_2$, EtOH, AcOH, 23 °C, quant.; (e) CDI, dioxane, reflux, 36 h, 55%; (f) TFA, CH_2Cl_2, 23 °C, 1.5 h, quant.

Table 1

Enzyme inhibitory activity for inhibitors **5a–g**

Entry	Inhibitor	K_i (nM)
1.	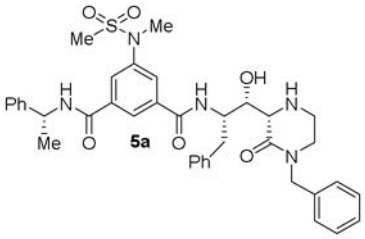	2.0
2.	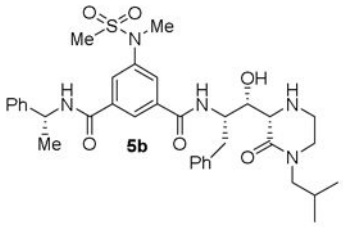	12.9
3.	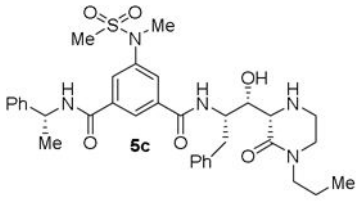	20.5
4.	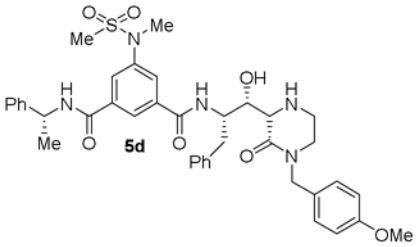	81.4
5.	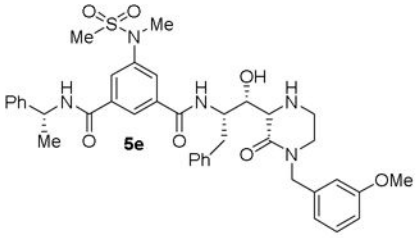	129

Entry	Inhibitor	K_i (nM)
6.	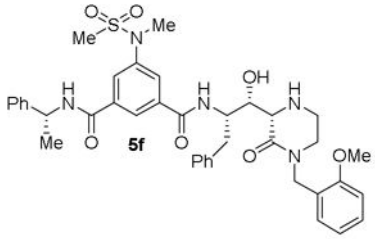 **5f**	144
7.	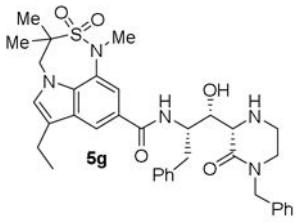 **5g**	67.1

Table 2

Enzyme inhibitory activity for inhibitors **6a–j**

Entry	Inhibitor	K_i (nM)
1.	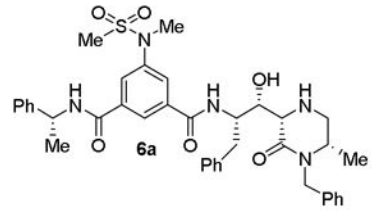	52900
2.	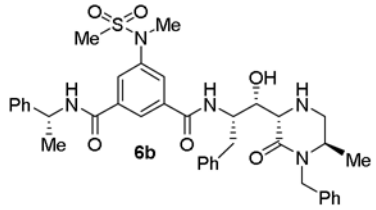	180
3.	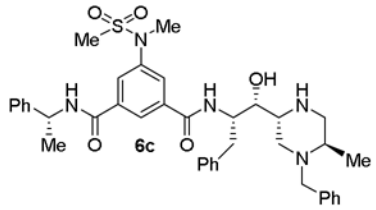	300
4.	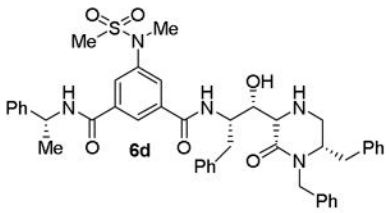	32600
5.	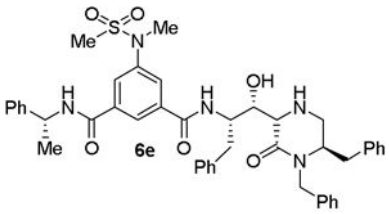	22200

Entry	Inhibitor	K_i (nM)
6.	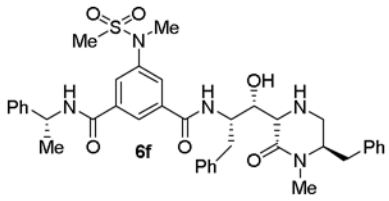	12
7.	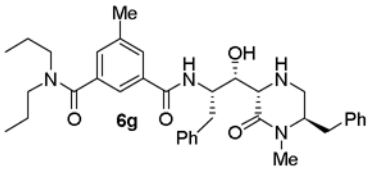	320
8.	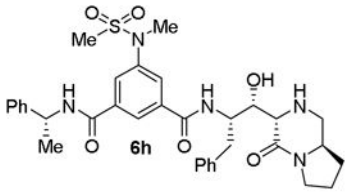	26
9.	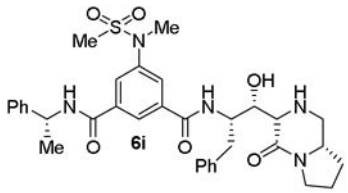	5690
10.	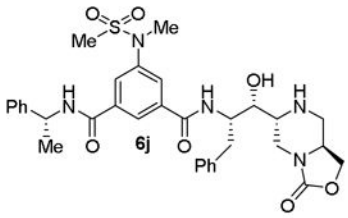	23